Limnol. Oceanogr., 35(4), 1990, 822–829

Realization of new production in coastal upwelling areas: A means to compare relative performance

R. C. Dugdale,[1] *F. P. Wilkerson,*[1] *and A. Morel*
Laboratoire de Physique et Chimie Marines, 06230 Villefranche-sur-Mer, France

Abstract

A theoretical basis for analyzing new production of upwelling centers under various conditions and for comparing the relative performance of different upwelling centers has been developed using the concept of shift-up or acceleration of NO_3^- uptake. NO_3^- concentration at the beginning of an upwelling cycle determines the rate of acceleration, the maximal specific NO_3^- uptake rate, and the maximal new production rate achieved. The relationship between initial NO_3^- concentration and new production rate is nonlinear and a doubling of initial NO_3^- concentration results in a threefold increase in new production. The tendency for new biomass to increase during an upwelling cycle varies widely between different upwelling regions and, by comparing theoretical predictions with data, the performance of an upwelling system can be judged against optimal expectations and the realization of potential new production by the system estimated. Among upwelling centers at Cap Blanc (northwest Africa), 15°S (off the coast of Peru), and Point Conception (California), the least of this potential is realized at Point Conception.

New production, that portion of the primary production based upon entry of new primary nutrient into the euphotic zone, is the basis for net transfer of CO_2 from the atmosphere to the ocean and of the transport of C to the deep ocean by sinking of particles (Eppley and Peterson 1979; Martin et al. 1987). One definition of new production is the productivity that results from the upward vertical flux of NO_3^- (Dugdale and Goering 1967) and consequently the uptake of that NO_3^- by phytoplankton. This flux proceeds relatively slowly over most of the oceans, more actively along the equatorial divergences, and very rapidly in coastal upwelling regions. It follows that the coastal upwelling regions also must contribute a disproportionately large share of global new production (Ryther 1969).

Examination and modeling of the entire productivity cycle occurring in a coastal upwelling system yields information necessary to understand the capacity for new production in the area. The changes in biological and nutrient processes with time as water drifts away from an upwelling center have been described by MacIsaac et al. (1985), Dugdale and Wilkerson (1985), and Wilkerson and Dugdale (1987). In a conveyor-belt type of scheme, upwelled phytoplankton adapt to high light and high nutrients at the surface, but at first there is little nutrient uptake due to small population size and low specific uptake rates. Farther downstream there are increases in NO_3^- uptake rates and population size, and eventually high uptake rates result in sudden nutrient depletion. Sinking out of phytoplankton (that can no longer take up nutrients) occurs at various points along the conveyor belt, although most sinking probably occurs when nutrients become fully depleted. This concept arose primarily from investigations at 15°S, off Peru, where an upwelling plume has been known to occur at the same location over most of the year (Gunther 1936; Zuta and Urquino 1972) and from studies at Point Conception, California (Wilkerson and Dugdale 1987; Dugdale and Wilkerson 1989), and is applicable to the upwelling center at Cape Town, South Africa, that develops a similar plume (Andrews and Hutchings 1980). It does not have rigid constraints and can be applied to regions where the location of maximal upwelling intensity

[1] Present address: Department of Biological Sciences, University of Southern California, Los Angeles 90089.

Acknowledgments

This study was supported by the French Centre National de la Recherche Scientifique (UA 353), National Science Foundation grant OCE87-10774, and NASA grant 161-30-33-40-55 to C. O. Davis.

We thank all those at CNRS and the Laboratoire de Physique et Chimie Marines for making this study possible.

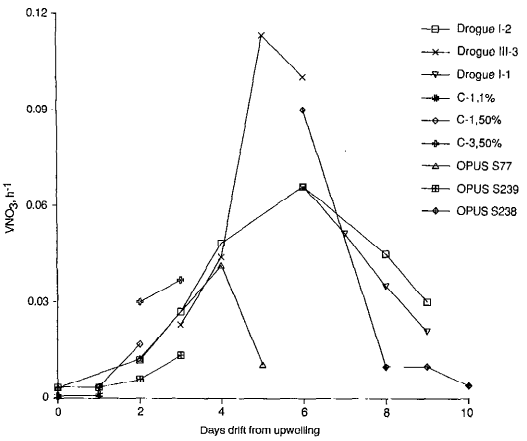

Fig. 1. Time-course of specific NO_3^- uptake rate in a series of hold-over and drifter- and drogue-following experiments. Drogue experiments I-2, III-3, and I-1 and hold-over experiments C-1 (1%), C-1 (50%), and C-3 (50%) were carried out at 15°S, off Peru, during the JOINT 2 cruise. (Details given by MacIsaac et al. 1985.) Drifter experiments OPUS S77, S239, and S238 were carried out at Point Conception, California. (Details given by Dugdale and Wilkerson 1989.)

Significant symbols

$[NO_3]$, $[NO_3]_t$, $[NO_3]_i$	NO_3^- concn, at time t, and at time 0 (μg-atoms N liter^{-1})
VNO_3	Biomass-specific NO_3^- uptake (h^{-1})
ρNO_3	NO_3^- uptake per unit volume (μg-atoms N liter^{-1})
PON	Particulate N concn (μg-atoms N liter^{-1})
A	Acceleration of NO_3^- uptake (h^{-2})
LPD	Light penetration depth (%)
t_f	Time to NO_3^- exhaustion (h)
r	Ratio of observed to theoretical maximum ρNO_3

varies with time along the coast or where lateral incorporation of phytoplankton by horizontal advection in addition to the upwelling may provide another "seed" source (Jones et al. 1988).

Drifter studies (Dugdale and Wilkerson 1985; MacIsaac et al. 1985; Wilkerson and Dugdale 1987) and shipboard hold-over experiments (MacIsaac et al. 1985) have followed phytoplankton in the vicinity of strongest upwelling and show low NO_3^- uptake that "shifts up" (Schaechter 1968; MacIsaac et al. 1974; Dugdale 1977) or accelerates and then "shifts down" as nutrients are depleted (Fig. 1). Shift-up besides being a function of time from upwelling (Fig. 1) is also related to the initial NO_3^- concentration (Wilkerson and Dugdale 1987). Zimmerman et al. (1987) incorporated the shift-up concept into a model of upwelling productivity by using an acceleration term and showed that shift-up from the low NO_3^- uptake values of the upwelling center must occur for the model to predict the observed productivity levels. We have developed this concept further and constructed a model designed to simulate the time-course of NO_3^- uptake (equivalent to new production) that would be seen by following a drifter tracking the productivity cycle from the site of upwelling downstream. This model differs in several ways from that of Zimmerman et al. (1987) but primarily by incorporating the shift-down side of the productivity cycle and considering irradiance to be saturating for uptake throughout the cycle. Using acceleration, A (defined in list of symbols), along with the initial conditions at the upwelling center and time from upwelling to exhaustion of the NO_3^- through phytoplankton growth, it predicts both specific NO_3^- uptake V and uptake liter^{-1} as a function of time. These variables plotted against each other provide a theoretical basis for evaluating the relative performance of upwelling systems in terms of biomass production.

Model description

Data used in developing the model were obtained during the JOINT 1 and CINECA 5 studies of the Cap Blanc region of northwest Africa in 1974 (e.g. Brink et al. 1981; MacIsaac et al. 1974; Dugdale and Wilkerson 1985; Groupe Mediprod 1976) during the Coastal Upwelling Ecosystems Analysis (CUEA) and Cooperative Investigations of the Northern part of the Eastern Central Atlantic (CINECA) programs, the Peru upwelling center at 15°S made during CUEA in 1976 and 1977 (MacIsaac et al. 1985; Wilkerson et al. 1987), and the Point Conception, California, upwelling center carried out in 1981 and 1983 (Jones et al. 1983, 1988; Atkinson et al. 1986; Wilkerson and Dugdale 1987; Dugdale and Wilkerson 1989) by the Organization of Persistent Upwelling Structures (OPUS) program. NO_3^- uptake measurements with ^{15}N as a tracer

and mass spectrometry (Dugdale and Wilkerson 1986) were made on all of the cruises to these regions, along with temperature, ^{14}C fixation, Chl *a*, nutrients, and many other biological variables.

The rate of NO_3^- uptake is expressed (Dugdale and Goering 1967) as either the biomass-specific NO_3^- uptake (V_{NO_3}) or as the assimilation rate of NO_3^- per unit volume of seawater, ρNO_3 respectively defined as

$$V_{NO_3} = \frac{1}{PON} \times \frac{dPON}{dt} \quad (1a)$$

and

$$\rho NO_3 = V_{NO_3} \times PON = dPON/dt \quad (1b)$$

where PON is the particulate organic N concentration (*see list of symbols*).

Newly upwelled phytoplankton progressively adapt to high light and nutrient at the surface. The result of such an adaptation is an increase of biomass-specific NO_3^- uptake from an initial low value $V_{NO_{3(i)}}$ (MacIsaac et al. 1985; Wilkerson and Dugdale 1987). Zimmerman et al. (1987) parameterized this effect by introducing the acceleration term A (with the units of h^{-2}) to describe this shift-up of V_{NO_3}, so that

$$V_{NO_{3(t)}} = V_{NO_{3(i)}} + At \quad (2)$$

with

$$A = dV_{NO_3}/dt \quad (3)$$

where (t) refers to a variable measured at a specific time and (i) to initial values ($t = 0$). $V_{NO_{3(i)}}$ is not necessarily identical to the V_{max} commonly associated with Michaelis-Menten kinetics, but rather represents the maximal value observed when $[NO_3]$ is not limiting. In addition, Zimmerman et al. showed that A is not a constant but depends in a linear way on the initial $[NO_3]$ in the upwelling center, $[NO_3]_i$, therefore

$$A = \alpha[NO_3]_i + \beta. \quad (4)$$

As a consequence of this equation, different upwelling centers with various nutrient concentrations of the source waters will experience shift-up of different intensities. The above set of equations accounts for the shift-up regime, which obviously is of limited duration. The specific rate V_{NO_3} cannot continue to increase with time (as predicted by Eq. 2) until the complete exhaustion of NO_3^- which would abruptly entail a null value for V_{NO_3}. Drifter and drogue data actually have shown that V_{NO_3} reaches a peak after ~4–6 d and then shifts down (Fig. 1). The decrease which coincides with progressively decreasing nutrient availability originates from the influence of substrate-limitation kinetics. Using Michaelis-Menten kinetics, we can express the nutrient-limited rate at a given time, t, as substrate-limited

$$V_{NO_{3\lim(t)}} = \frac{V_{NO_{3(i)}}[NO_3]_t}{K_s + [NO_3]_t} \quad (5)$$

where K_s is the half-saturation constant in μg-atoms N liter^{-1}. To establish $V_{NO_{3\lim(i)}}$, we consider that $V_{NO_{3(i)}}$ is that value computed through Eq. 2 which ignores the nutrient limitation. Note that use of Eq. 5 implies that the temporal evolution of the $[NO_3]$, $[NO_3]_t$, is assessed. Within the frame of the adopted hypotheses, the consumption of NO_3^- is balanced by the accumulation of PON, so that symmetrical expressions describe the time-course of $[NO_3]$ and PON

$$[NO_3]_t = [NO_3]_i - \int_i^t \rho NO_{3(t)}\, dt \quad (6a)$$

$$[PON]_t = [PON]_i + \int_i^t \rho NO_{3(t)}\, dt \quad (6b)$$

where ρNO_3 (*see Eq. 1b*) is itself a function of time.

With Eq. 1a, 1b, 2, 4, and 5 and an Euler integration we calculated the time-course of biomass-specific NO_3^- uptake for various values of $[NO_3]_i$ ranging from 5 to 30 μg-atoms liter^{-1}. The family of curves is shown in Fig. 2; starting from the same initial value ($5 \times 10^{-3}\ h^{-1}$), the initial slopes of the curves are proportional to the values of $[NO_3]_i$. The decline that is shown in all of the curves between 48 and 72 h is the result of the depletion of NO_3^-. In the absence of limitation of uptake by the ambient concentration, this decline should be a sudden fall as shown by the dashed line in Fig. 2. Increasing the Michaelis-Menten constant K_s results in a smoothing effect of the V_{NO_3} max-

imum, which marks the transition between the shift-up and shift-down phases and also results in a lengthening of the shift-down regime. Everything being kept constant, the time elapsed for complete exhaustion (and null uptake) is inversely related to the value adopted for term A (Eq. 4). With the K_s as adopted, the decline in V_{NO_3} occurs in a relatively narrow band of time regardless of the $[NO_3]_i$ value (note that higher initial concentrations are more quickly consumed). The various shapes of the curves derived from field experiments (Fig. 1) reflect the possible impact of the above parameters, K_s, A, and $[NO_3]_i$.

In the absence of Michaelis-Menten limitation, $V_{NO_{3(t)}}$ and $\rho NO_{3(t)}$ can be simply computed as a function of time until complete consumption of the substrate. From the definition of ρNO_3 (Eq. 1b) combined with Eq. 2, it follows that

$$\frac{dPON}{PON_{(t)}} = [V_{NO_{3(i)}} + At]\, dt,$$

which after integration yields

$$PON_{(t)} = PON_{(i)} \exp[V_{NO_{3(i)}} t + At^2/2] \quad (7)$$

where $PON_{(i)}$ is the initial value at $t = 0$. The time until exhaustion, t_f, is determined when

$$PON_{(t_f)} - PON_{(i)} = [NO_3]_i,$$

and finally $\rho NO_{3(t)}$, obtained as the product of $V_{NO_{3(t)}}$ with $PON_{(t)}$, is

$$\rho NO_{3(t)} = [V_{NO_{3(i)}} + At]PON_{(i)} \cdot \exp[V_{NO_{3(i)}} t + At^2/2]. \quad (8)$$

The shape of the ρNO_3 vs. V_{NO_3} curves, computed for different initial NO_3^- values is shown in Fig. 3. These curves rise steeply since PON is exponentially increasing. The upper endpoints of the curves indicate the maximal values of both V_{NO_3} and ρNO_3 that could be expected in upwelling areas with the indicated starting $[NO_3]$. These values are maximal to the extent that the effect of decreasing $[NO_3]$ on uptake is considered as not limiting, and also because the biomass progressively formed (Eq. 7) is able to accumulate (e.g. no loss, no grazing). If it is conversely assumed that there is no accumulation, with $PON_{(t)}$ remaining equal to $PON_{(i)}$, the curves in Fig. 3 degenerate into a single straight line with a slope equal to $PON_{(i)}$ (straight line). This line can be seen as the lower limit to be observed if the products of the primary production were instantaneously exported toward other physical (depth) or trophic levels. The time for $[NO_3]$ exhaustion (t_f) and the maximal attainable values of V_{NO_3} and ρNO_3 at t_f are shown as a function of the initial $[NO_3]$ at the upwelling center (Fig. 4). The ρNO_3 curve (Fig. 4c) is gently concave upward and thus emphasizes the multiplicative effect of increasing $[NO_3]_i$; for instance, doubling $[NO_3]_i$ from 15 to 30 μg-atoms liter^{-1} results in a nearly threefold increase in the maximal new production rate, whereas V_{NO_3} is only multiplied by about 1.6. This result is a consequence of the biomass accumulating in a live form and remaining able to incorporate N from NO_3^-.

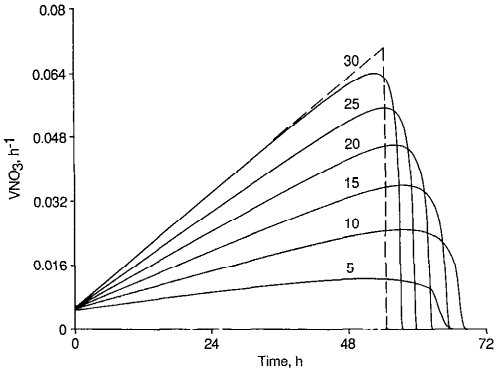

Fig. 2. Theoretical time-course of specific NO_3^- uptake, V_{NO_3}, for a series of initial $[NO_3]$. The parameter α and β in Eq. 4 are both given the values 4×10^{-5} (*see* Zimmerman et al. 1987). The dashed line is 30 μg-atoms liter^{-1} and no Michaelis-Menten limitation, whereas the curves (for $[NO_3]$ as indicated) include a Michaelis-Menten effect (with $K_s = 1$ μg-atom liter^{-1}).

Comparison of model results with data

The values of $V_{NO_{3(i)}}$, $PON_{(i)}$, and $[NO_3]_i$ for the most active upwelling locations for the three different study areas (Table 1) were used for initial boundary conditions in the shift-up model to simulate $\rho NO_{3(t)}$ vs. $V_{NO_{3(t)}}$ relationships for comparison with shipboard measurements of ρNO_3 and V_{NO_3} with ^{15}N. Initial PON values for each region were quite similar, although values of initial

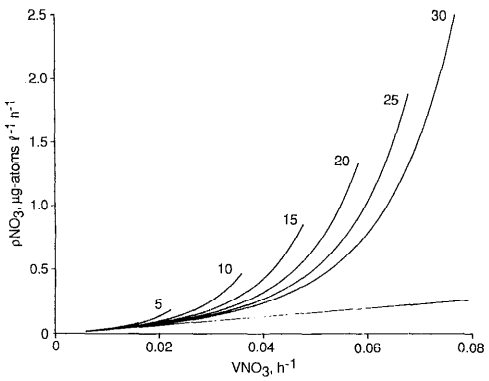

Fig. 3. Modeled relationship (in absence of Michaelis-Menten kinetics) between the assimilation rate, ρNO_3 (new production) and biomass-specific NO_3^- uptake rate, VNO_3, for a series of initial $[NO_3]$ in upwelled waters. The upper end of each curve represents the conditions when all NO_3^- has been incorporated as N into the living particulate pool. The straight line indicates the ρNO_3 evolution with no accumulation of biomass as PON. For all computations $PON_{(i)}$ is set equal to 3 μg-atoms liter^{-1} and $VNO_{3(i)}$ is 0.005 h^{-1}.

$[NO_3]$, initial VNO_3, and A were considerably higher off Peru, compared to Cap Blanc and Point Conception. The ρNO_3 vs. VNO_3 relationships were simulated for two theoretical situations (Figs. 5–7) in which either all NO_3^- taken up from these conditions accumulates as biomass (curved lines) or in which there is no accumulation (straight lines). The upper end of the curved lines indicates the maximum possible VNO_3 and ρNO_3 for the initial values of VNO_3 and $[NO_3]$.

The ^{15}N data from the JOINT 1 cruise to Cap Blanc fall above the "no accumulation" line of the model, with a tendency to accumulate PON, although some points at higher VNO_3 indicate less than complete PON accumulation (Fig. 5). The maximum value of new production, ρNO_3, was not high, 0.4 μg-atom liter^{-1} h^{-1}, probably due to the low NO_3^- conditions of the North Atlantic that limit VNO_3 to a maximum of 0.04 h^{-1}.

The 15°S data from the 1977 JOINT 2 productivity stations show a clear tendency for accumulation of biomass, compared with model results using initial conditions for the three drifters (Table 1), with values of new production reaching to 0.65 μg-atom liter^{-1} h^{-1} (Fig. 6). Most data points lie between the curve for drifter I-2, which exhibited a low accumulation rate, and the no-accumulation line. Maximal values of VNO_3,

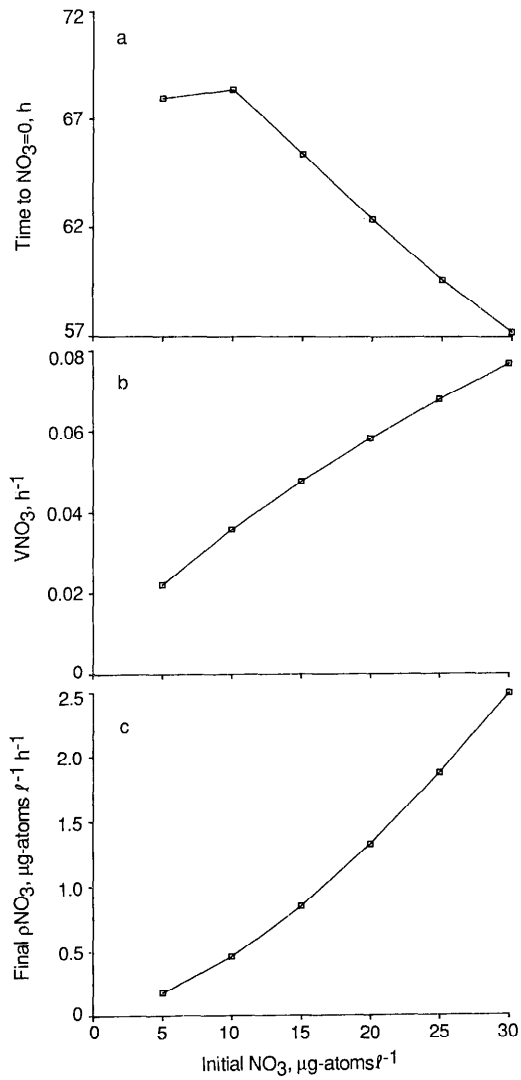

Fig. 4. The time for $[NO_3]$ exhaustion and the final maximal values of VNO_3 and ρNO_3 plotted as a function of the initial $[NO_3]$ in the upwelling center.

0.095 h^{-1} are >2 times higher than observed at the Cap Blanc upwelling center.

The initial values at location G-1 (the station closest to the Point Conception upwelling source and where drifters were deployed) for the S77 drifter were used to compute the upper accumulation curve shown in Fig. 7. Comparison of the full data set of $^{15}NO_3^-$ uptake data from productivity stations taken during OPUS 1983 with the theoretical lines calculated with S77 drifter values (Table 1) shows (Fig. 7) that the Point Conception upwelling center did not accu-

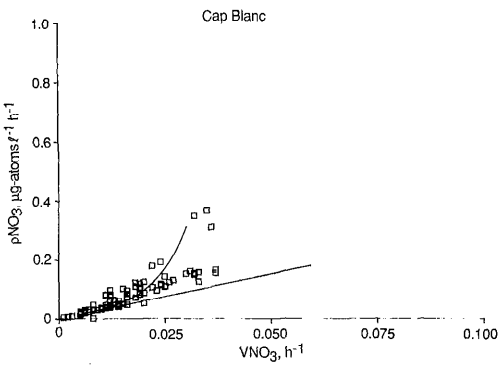

Fig. 5. New production rate vs. specific NO_3^- uptake rate for the Cap Blanc upwelling region. Data from ^{15}N measurements—□. Curved line is the theoretical relationship when all NO_3^- taken up is retained as biomass (as in Fig. 3) using the initial conditions from Table 2. Straight line is the case when no biomass accumulation occurs, i.e. PON is constant and equal to initial PON.

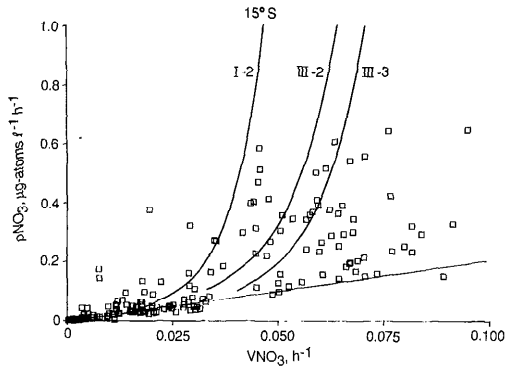

Fig. 6. As Fig. 5, but for the upwelling center at 15°S. Data from the JOINT 2 study in 1977.

mulate phytoplankton biomass and consequently had only relatively low values of new production (0.3 µg-atom liter^{-1} h^{-1}), even though maximal V_{NO_3} values were high (0.1 h^{-1}). This high V_{NO_3} is due to high initial $[NO_3]$ (up to 23 µg-atoms liter^{-1}).

Discussion

A basis of the shift-up model is that maxima of V_{NO_3} and initial nutrient concentrations are positively related. The relationship between ρNO_3 arising from the model and initial $[NO_3]$ suggests a nonlinear increase in maximal ρNO_3 with $[NO_3]_i$. The initial NO_3^- values given in Table 1 for the three regions were used to calculate the maximal ρNO_3 expected. Calculated values and the maximum observed values are shown in Table 2, along with r (the ratio of observed to calculated maximum values) that can be considered to be a measure of the degree to which potential new production is realized. Cap Blanc has the highest realization of potential production because r is practically unity (within the expected accuracy in such computations); Peru is second with $r = 0.6$ and Point Conception with $r < 0.2$ would

Table 1. Initial conditions at upwelling centers sampled at the 50 and 100% light penetration depths (LPD).

Upwelling region	Drifter*	LPD (%)	V_{NO_3} (h^{-1})	PON (µg-atoms N liter^{-1})	NO_3^- (µg-atoms N liter^{-1})	A† ($h^{-2} \times 10^{-4}$)
Cap Blanc, 1974		100	0.0063	2.98	7.4	
		50	0.0099	3.15	7.2	
		mean	0.0080	3.06	7.3	
15°S, 1977	I-2	100	0.0107	2.09	24.8	5.5
		50	0.0118	2.05	24.8	3.2
		mean	0.0112	2.07	24.8	
	III-2	100	0.0399	3.82		
		50	0.0261	2.46	22.5	15.8
		mean	0.0330	3.14		
	III-3	100	0.0276	1.37	23.6	12.4
		50	0.0530	3.72	23.7	
		mean	0.0403	2.54	23.6	
Pt. Conception, 1983	S77	100	0.0068	2.93	15.0	3.8
		50	0.0048	3.36	15.0	
		mean	0.0058	3.14	15.0	
	S239	100	0.0022	3.42	10.1	1.2
		50	0.0034	2.71	9.9	
		mean	0.0028	3.06	10.0	

* Cap Blanc values from 15 midshelf stations with depths <50 m, Peru and Point Conception data initiated at station closest to upwelling center.
† Acceleration calculated from V_{NO_3} values from day 0 to day 1 for Peru and from day 1 to day 2 for Point Conception.

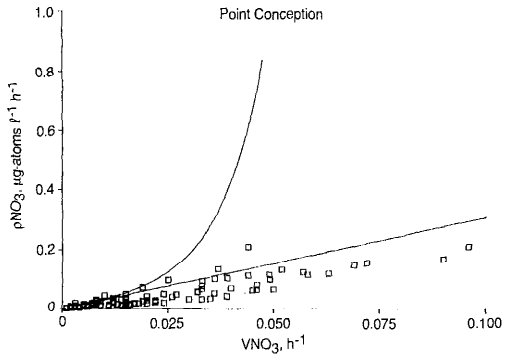

Fig. 7. As Fig. 5, but for the Point Conception upwelling center during the 1983 OPUS study.

be much less efficient. The northwest Africa and Peru systems appear reasonably close to realizing maximal potential new production rates. The low value for Point Conception results from the lack of biomass accumulation, as indicated in Fig. 7.

The theory and analysis presented here allow the performance of an upwelling system to be examined by looking at both the specific (V_{NO_3}) and absolute (ρNO_3) NO_3^- uptake rates. The behavior of specific uptake rates appears to be a function of $[NO_3]$ and time. A distinction should be made, however, between the specific uptake rates as measured and specific uptake rates as they may occur at the phytoplankton cellular level. The measured rates are diluted to the extent that nonliving, nonphytoplankton particulate N is present in the sample when analyzed for ^{15}N. The measured specific uptake rates were used in model development, and the model reflects actual ^{15}N measurements. The model is useful within these limits in comparing the behavior of different upwelling regions or in assessing variability within a specific upwelling region.

An examination of ρNO_3 as a function of V_{NO_3} also provides an assessment of the ability of the system to accumulate biomass, i.e. to "bloom." In this study, high initial $[NO_3]$ usually resulted in high specific uptake rates, but high new production rates were not always realized. Minas et al. (1986) computed new production rates for northwest African, Peruvian, and southwest African upwelling regions based on chemical and hydrographic fields with time since upwelling calculated from heating rates. The

Table 2. Calculated *r* (realization of new production) for three upwelling centers.

Upwelling region	Max ρNO_3 (μg-atoms liter^{-1} h^{-1}) Observed	Max ρNO_3 (μg-atoms liter^{-1} h^{-1}) Theoretical	*r*	Initial $[NO_3]$ (μg-atoms N liter^{-1})
Cap Blanc, 1974*	0.36	0.30	1.2	7.36
15°S, 1977†	0.57	0.95	0.6	24.80
Pt. Conception, 1983‡	0.21	0.85	0.2	15.00

* RV *Atlantis-2*, JOINT 1 cruise data.
† RV *Wecoma*, JOINT 2 cruise data.
‡ RV *Velero IV*, OPUS 1983 cruise data.

northwest African region showed high production rates with a short time to nutrient exhaustion, in accord with our measurements and model results. A model of the Peruvian upwelling plume at 15°S (Walsh and Dugdale 1971) described biomass accumulation, with full depletion of NO_3^- in 5–9 d of drift from the upwelling center. In contrast to our results, Minas et al. (1986) found Peru to have low mean new production rates and very long times to nutrient exhaustion. Their computations were based on heat input rates that were relatively low but appropriate for cloudy periods of the year rather than for the relatively clear periods of March–April during which our data were obtained. Our data from Point Conception showed low growth rate and low biomass accumulation with a long time scale. The reasons for the lack of accumulation of biomass in spite of high specific uptake rates are not clear but include high advective rates that may place the high biomass region outside of the study area, high sinking rates, and strong grazing pressure. As more data from the major upwelling regions accumulate, these areas will be seen to exhibit both accumulation and nonaccumulation modes. The constraints of characteristic nutrient concentrations of the source waters can be expected to hold, however, with each region exhibiting characteristic maxima in both V_{NO_3} and ρNO_3 but with considerable annual and interannual variability.

References

ANDREWS, W. R. H., AND L. HUTCHINGS. 1980. Upwelling in the Southern Benguela Current. Prog. Oceanogr. **9**: 1–81.

ATKINSON, L. P., AND OTHERS. 1986. Mesoscale hydrographic variability in the vicinity of Points Conception and Arguello during April–May 1983: The OPUS 1983 experiment. J. Geophys. Res. **91:** 12,899–12,918.

BRINK, K. H., AND OTHERS. 1981. Physical and biological structure and variability in an upwelling center off Peru near 15°S during March, 1977, p. 473–496. *In* F. A. Richards [ed.], Coastal upwelling. Am. Geophys. Union.

DUGDALE, R. C. 1977. Nutrient modeling, p. 789–806. *In* E. D. Goldberg et al. [eds.], The sea. V. 6. Wiley.

———, AND J. J. GOERING. 1967. Uptake of new and regenerated forms of nitrogen in primary productivity. Limnol. Oceanogr. **12:** 196–206.

———, AND F. P. WILKERSON. 1985. Primary production in the Cap Blanc region. Int. Symp. Upwelling. W. Africa, Inst. Invest. Pesq., Barcelona **1:** 233–243.

———, AND ———. 1986. The use of ^{15}N to measure nitrogen uptake in eutrophic oceans; experimental considerations. Limnol. Oceanogr. **31:** 673–680.

———, AND ———. 1989. New production in the upwelling center at Point Conception, California: Temporal and spatial patterns. Deep-Sea Res. **36:** 985–1007.

EPPLEY, R. W., AND B. J. PETERSON. 1979. Particulate organic matter flux and planktonic new production in the deep ocean. Nature **282:** 677–680.

GROUPE MEDIPROD. 1976. Résultats des campagnes a la mer No. 10, CINECA 5 Cruise Rep. CNEO, Brest.

GUNTHER, E. R. 1936. A report on oceanographical investigations in the Peru Coastal Current. Discovery Rep. **13:** 107–276.

JONES, B. H., L. P. ATKINSON, D. BLASCO, K. H. BRINK, AND S. L. SMITH. 1988. The asymmetric distribution of chlorophyll associated with a coastal upwelling center. Cont. Shelf Res. **8:** 1155–1170.

———, AND OTHERS. 1983. Observations of a persistent upwelling center off Point Conception, California, p. 37–60. *In* E. Suess and J. Thiede [eds.], Coastal upwelling. Part A. Plenum.

MACISAAC, J. J., R. C. DUGDALE, R. T. BARBER, D. BLASCO, AND T. T. PACKARD. 1985. Primary production cycle in an upwelling center. Deep-Sea Res. **32:** 503–529.

———, ———, AND G. SLAWYK. 1974. Nitrogen uptake in the northwest African area: Results from CINECA-CHARCOT II cruise. Tethys **6:** 69–76.

MARTIN, J. H., G. A. KNAUER, D. M. KARL, AND W. W. BROENKOW. 1987. VERTEX: Carbon cycling in the northeast Pacific. Deep-Sea Res. **34:** 267–285.

MINAS, H. J., M. MINAS, AND T. T. PACKARD. 1986. Productivity in upwelling areas deduced from hydrographic and chemical fields. Limnol. Oceanogr. **31:** 1182–1206.

RYTHER, J. H. 1969. Photosynthesis and fish production in the sea. Science **166:** 72–76.

SCHAECHTER, M. 1968. Growth: Cells and populations, p. 136–162. *In* J. Mandelstam and K. McQuillen [eds.], Biochemistry of bacterial growth. Wiley.

WALSH, J. J., AND R. C. DUGDALE. 1971. A simulation model of the nitrogen flow in the Peruvian upwelling region. Invest. Pesq. **35:** 309–331.

WILKERSON, F. P., AND R. C. DUGDALE. 1987. The use of large shipboard barrels and drifters to study the effects of coastal upwelling on phytoplankton nutrient dynamics. Limnol. Oceanogr. **32:** 368–382.

———, ———, AND R. T. BARBER. 1987. Effects of El Niño on new, regenerated and total production in eastern boundary upwelling systems. J. Geophys. Res. **92:** 14,347–14,353.

ZIMMERMAN, R. C., J. N. KREMER, AND R. C. DUGDALE. 1987. Acceleration of uptake by phytoplankton in a coastal upwelling ecosystem: A modeling analysis. Limnol. Oceanogr. **32:** 359–367.

ZUTA, S., AND W. URQUINO. 1972. Temperatura promedio de la superficie del mar frente a la costa Peruana periodo 1928–1969. Bol. Inst. Mar Peru **2:** 459–520.

Submitted: 22 March 1989
Accepted: 6 November 1989
Revised: 26 February 1990